Tectonic and sedimentary evolution of the Cenozoic Hatay Graben, Southern Turkey: a two-phase model for graben formation

SARAH J. BOULTON[1], ALASTAIR H. F. ROBERTSON[1] & ULVI C. ÜNLÜGENÇ[2]

[1]*School of GeoSciences, Grant Institute, Edinburgh University, Edinburgh EH9 3JW, UK (e-mail: sarah.boulton@glg.ed.ac.uk)*

[2]*Department of Geological Engineering, Çukurova University, Balcali, 01330 Adana, Turkey*

Abstract: New structural and sedimentary studies form the basis of a new interpretation for the Neogene Hatay Graben. Fault analysis reveals three contemporaneous trends of fault orientation (000°–180°, 045°–225° and 150°–350°) suggesting that the graben is transtensional in nature. Sedimentary studies show that, following shallow-marine deposition from the Late Cretaceous to the Eocene, a hiatus ensued until Early Miocene fluvial sedimentation. After a Mid-Miocene marine transgression, water depths increased until the Messinian salinity crisis, followed by a regression from the Pliocene to the present day. The basin initially developed as the distal margin of a foreland basin of the Tauride allochthon to the north, developing a classic sedimentary sequence during Mid–Late Miocene. Stresses caused by loading of the crust created a flexural forebulge to the south that supplied sediment mainly northwards. During the Plio-Quaternary, transtensional graben development took place, primarily influenced by the westward tectonic escape of Anatolia along the East Anatolia Fault Zone and left-lateral offset along the northward extension of the Dead Sea Transform Fault. This area is, thus, an excellent example of a foreland basin reactivated in a strike-slip setting. Our new two-phase model: foreland basin, then transtensional basin for the Hatay Graben, is in contrast to previous models, in which it was generally assumed that the Plio-Quaternary Hatay Graben represents a direct extension of the Dead Sea Fault Zone or the East Anatolian Fault Zone.

The Hatay region is located in the Eastern Mediterranean, near the border between Turkey and Syria (Fig. 1). This is an area of active neotectonics where three major structural lineaments intersect: the southeastern end of the East Anatolian Fault Zone (EAFZ), the northern end of the Dead Sea Fault Zone (DSFZ) and the Cyprus Arc (Perinçek & Çemen 1990; Robertson 1998*b*). This study focuses on a prominent graben that trends NE–SW from near the town of Antakya to the Mediterranean Sea. This area was previously considered as an extension of a graben, variously known as the Hatay Graben (Perinçek & Çemen 1990), the Amanos Fault Zone (Lyberis *et al.* 1992), or the Karasu Rift (Lovelock 1984; Westaway 1994; Rojay *et al.* 2001; Över *et al.* 2002), and appears to link the EAFZ with the DSFZ through the Amik Plain (Fig. 1). Here, we apply the term Karasu Rift to the graben that trends northwards from the Amik Plain, whereas we will refer to our study area to the SW as the Hatay Graben.

The structural complexity of this area has led to a number of different tectonic interpretations. Tinkler *et al.* (1981) and Parlak *et al.* (1998) considered the Karasu Rift as a northward continuation of the DSFZ, whereas Arpat & Şaroğlu (1972) saw the EAFZ as a whole as a continuation of the DSFZ. Hempton (1987), Perinçek & Çemen (1990) and Westaway (1994) argued that the EAFZ runs from Karlıova to a position to the north of Cyprus and that it is not connected to the DSFZ. Others considered the Karasu Rift to be an extension of the EAFZ, which continues through the Hatay Graben and then offshore (Şengör *et al.* 1985; Lyberis *et al.* 1992; Şaroğlu *et al.* 1992), and thus separate from the DSFZ. In addition, Yürür & Chorowicz (1998) viewed the Karasu Rift as a separate structure from both the EAFZ and DSFZ.

Each of these tectonic interpretations was proposed following work mainly on the EAFZ and the DSFZ. To date, research on the Hatay Graben (Delaloye *et al.* 1980; Tinkler *et al.* 1981; Pişkin *et al.* 1986; Robertson 1986; Pirazzoli *et al.* 1991; Safak 1993*a,b*; Over *et al.* 2002) and on the Karasu Rift (Parlak *et al.* 1998; Rojay *et al.* 2001; Yurtmen *et al.* 2002; Över *et al.* 2004) has mainly focused on the regional tectonic setting and significance, whereas the sedimentary and

From: ROBERTSON, A. H. F. & MOUNTRAKIS, D. (eds) 2006. *Tectonic Development of the Eastern Mediterranean Region*. Geological Society, London, Special Publications, **260**, 613–634.
0305-8719/06/$15.00

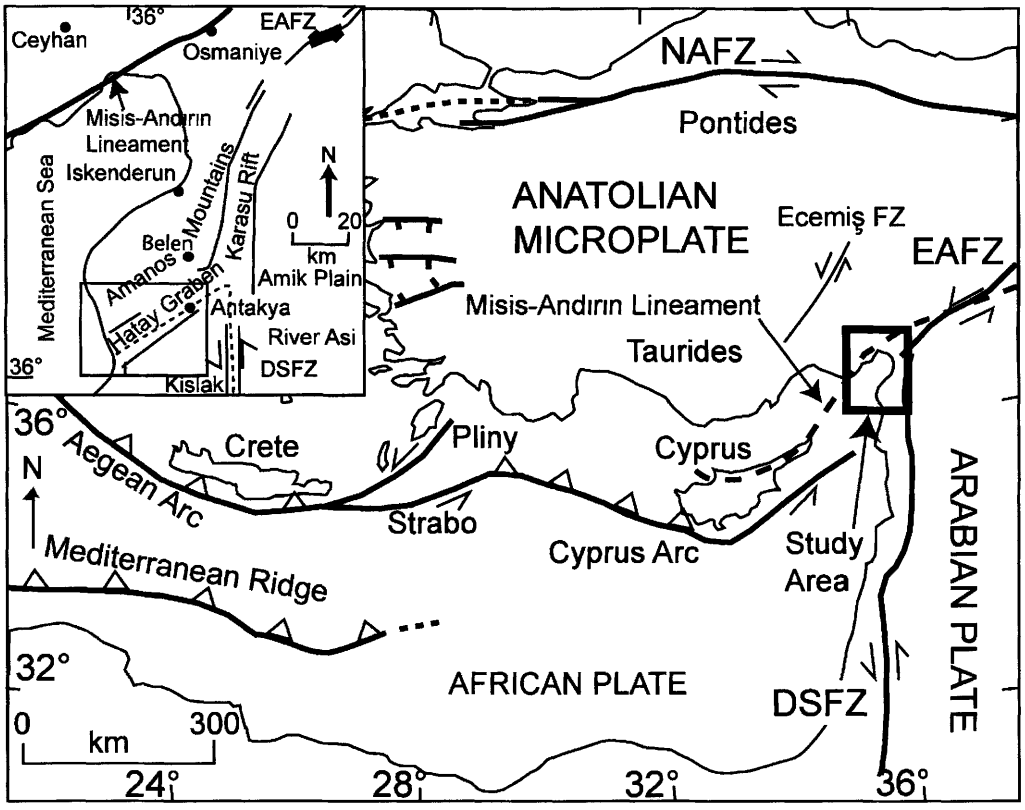

Fig. 1. Regional tectonic setting of the Eastern Mediterranean; the box shows the location of the inset map. Inset: outline map of the Hatay region, southern Turkey, showing major structures and some locations referred to in the text; box shows the location of Figure 2.

structural processes involved and the overall tectonosedimentary evolution have received little attention.

In this study we have investigated the evolution of the Hatay Graben, utilizing new sedimentological and structural studies to test existing models, and if appropriate develop a new one. We will show that the existing models are inadequate. The formation of the Hatay Graben predates the formation of the EAFZ, NAFZ and the northern DSFZ. The area was first part of the foreland basin to the Bitlis suture zone and normal faulting began during the Mid-Miocene, we suggest, as a result of isostatic loading. Following the cessation of continental collision in SE Turkey, strike-slip faulting and transtension become important in the Mid-Miocene and led to the formation of the present Hatay Graben. The Hatay Graben is an excellent example of a basin that has been dissected by normal faults in a foreland basin setting and later involved in strike-slip tectonics related to regional tectonic escape, in this case Anatolia westwards towards the Aegean Arc.

Regional geological setting

The post-Cretaceous tectonics of the Eastern Mediterranean region has resulted from the relative motions of the African, Arabian and Eurasian plates (McKenzie 1978). The northward motion of Africa and Arabia towards Eurasia has caused convergence and the emplacement of allochthonous units since the Late Cretaceous along what is now the Bitlis Suture Zone (McKenzie 1978; Şengör *et al.* 1985; Robertson 1998*a*). A foreland basin developed in SE Turkey along the Arabian margin parallel to the convergence front in Early–Mid Miocene time (Yılmaz 1993; Derman *et al.* 1996; Robertson 1998*a*, 2002). Continuing north–south-directed compression, as result of the motion of the Arabian plate, led to the uplift and crustal thickening

of Anatolia (Şengör & Kidd 1979) during Late Miocene–Quaternary time. By the Early Pliocene compressional tectonics were replaced by the westward extrusion of the Anatolian microplate along the dextral NAFZ, and the sinistral EAFZ (Fig. 1) (McKenzie 1978). These two strike-slip faults meet at a triple junction near the town of Karlıova in Eastern Turkey (Şengör *et al.* 1985; Bozkurt 2001). The NAFZ developed during the Mid-Miocene (McKenzie 1978; Şengör *et al.* 1985, 2005) to Late Miocene–earliest Pliocene (Barka *et al.* 2000) and is moving at around 15–25 mm a^{-1} (Oral *et al.* 1995; Reilinger *et al.* 1997). The initiation of the EAFZ is variously dated as Late Miocene to Early Pliocene (Şengör *et al.* 1985; Dewey *et al.* 1986; Hempton 1987), Late Pliocene (Şaroğlu *et al.* 1992), 3 Ma (Early Pliocene; Westaway & Arger 1996), or 1.8 Ma (Late Pliocene; Yürür & Chorowicz 1998). Global positioning system (GPS) measurements indicate that the current rate of slip along the EAFZ is 11 ± 2 mm a^{-1} (Reilinger *et al.* 1997). The relative motion between the African and Arabian plates is accommodated by sinistral motion along the DSFZ (Mart & Rabinowitz 1986; Chaimov *et al.* 1990; Beydoun 1999). The DSFZ links the rifted plate margin in the Red Sea to the convergent Bitlis suture zone in Southern Turkey (Hempton 1987). The southern DSFZ is considered to have formed as a result of the rifting of Arabia from Africa at *c.* 18–20 Ma (Garfunkel 1981; Hempton 1987; Lyberis 1988; Rojay *et al.* 2001), possibly in two stages, with the second phase and formation of the northern strands of the DSFZ beginning at *c.* 4.5 Ma: Early Pliocene (Freund *et al.* 1968; Girdler & Styles 1978; Brew *et al.* 2001). A further regionally important strike-slip lineament, the Ecemiş Fault Zone, to the NE of the study area (Fig. 1), is considered to show a left-lateral offset of *c.* 60 km mainly since Mid-Miocene time (Yetiş 1978; Koçyiğıt & Beyhan 1998; Jaffey & Robertson 2001). Much early displacement of Anatolia was accommodated along this lineament, prior to the Plio-Quaternary activity of the EAFZ.

Sedimentary evolution of the Hatay Graben

The topographic basin representing the Hatay Graben runs NNE–SSW from the present-day coast to the north of Antakya city (Figs 1 and 2). The basin has two well-defined topographic margins, which we refer to as the NW and SE margins, respectively. The SE margin exhibits a high topographic relief and is deeply incised by Quaternary streams, compared with the NW margin, which has a lower topographic relief. Near the coast, Quaternary river channel incision has resulted in exposures of Neogene sediments, especially as river terraces. Sedimentary units are exposed on both of the margins and in the axis of the Hatay Graben, ranging in age from the Late Cretaceous to Quaternary (Safak 1993*a*,*b*; Pişkin 1986; Fig. 2).

Late Cretaceous and Eocene (Kişlak and Okçular Formations, Table 1.1)

In the SE, the Hatay ophiolite is overlain by a sequence of latest Cretaceous (Maastrichtian) to Mid-Eocene (Lutetian) carbonates. Latest Cretaceous facies are generally grey, medium-bedded (beds generally 20–50 cm thick) wavy and convolute laminated shallow-marine microbial limestones with common secondary chert. In the south, the Eocene carbonates are composed of fine-grained, pale grey to pink limestones that contain abundant large benthic Foraminifera (e.g. *Nummulites* sp.), suggesting a water depth of 20–100 m (Saller *et al.* 1993). Further north, Eocene limestones include graded calcarenites with parallel and cross-lamination. The bases of some individual beds are erosional with scour marks; these limestones are interpreted as mainly relatively high-density calcareous turbidites. Latest Cretaceous and Eocene sediments accumulated regionally on the northern margin of the Arabian platform (Rigo de Righi & Cortesini 1964; Yılmaz 1993). During the latest Cretaceous, shallow-marine conditions persisted (0–50 m water depth) and microbial mats formed creating wavy laminated stromatolites that accumulated in the inner intertidal zone. During the Eocene, shelf carbonates rich in benthic Foraminifera accumulated in the SE; water depths increased to an estimated >100 m further NW, where hemipelagic carbonates and carbonate turbidites accumulated on a slope setting. The Oligocene was a period of non-deposition during which Eocene and older strata were folded and uplifted. Sedimentation resumed during Early Miocene (Aquitanian) time above an angular unconformity.

Early Miocene (Balyatağı Formation; Fig. 3, Table 1.1)

Lower Miocene sediments crop out along both of the present margins of the basin but only in the NE of the area (Fig. 3). Along the SE margin, matrix- and clast-supported, polymict conglomerates unconformably overlie Eocene limestones. The contact is occasionally marked by a carbonate interval (*c.* 2 m thick), rich in shallow-marine bivalves and bored pebbles (e.g. Harbiye area;

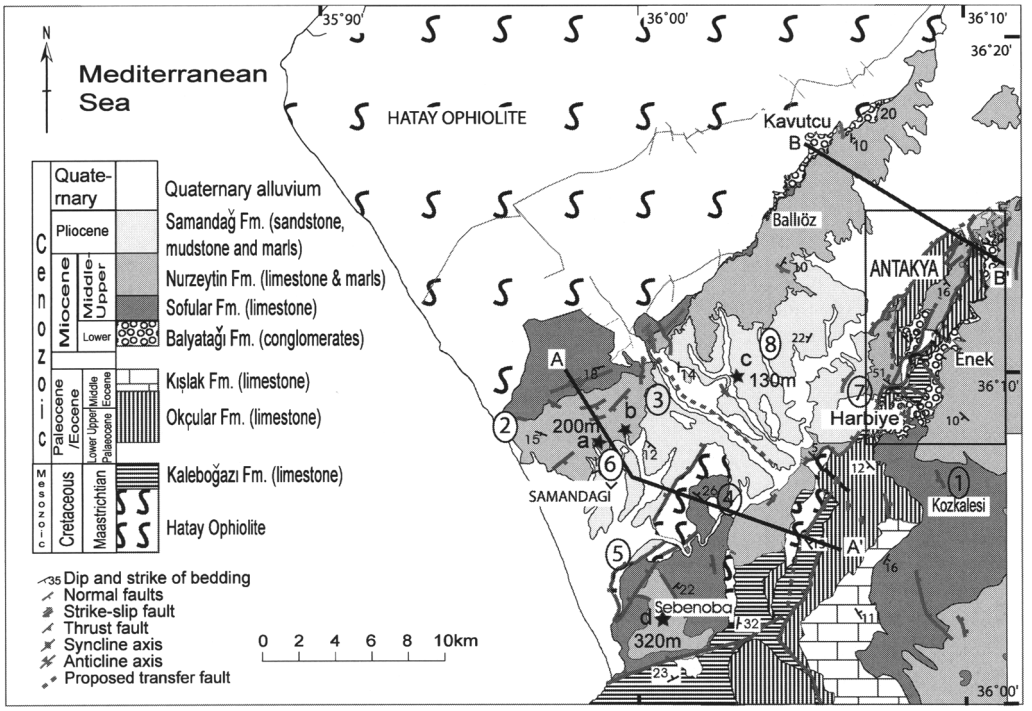

Fig. 2. Geological map of the Hatay Graben, southern Turkey. Lines indicate positions of cross-sections (Fig. 8) and box indicates location of Figure 5 (palaeocurrent map). Stars indicate the location and present altitude of Messinian evaporite deposits; letters refer to locations described in the text. Numbers in circles refer to localities in the text where evidence for synsedimentary faulting was observed. Based on data collected during this study, and on the work of Pişkin (1986) and Turkish masters degree students (especially A. Kop, T. Mistik and N. Temizhan).

Fig. 2). The conglomerates in the lower part of the formation are thick bedded, whereas higher in the sequence coarse conglomerates occur as lenses (tens of metres wide) within medium-grained sandstone, to conglomerate. Clastic sediments at the top of the formation exhibit pebble imbrication, large-scale cross-bedding and well-developed palaeosols (Fig. 4a). Figure 5 shows palaeocurrent measurements, based on clast imbrication and cross-bedding, as recorded along the SE basin margin. The current flow was generally to the north to NE (0°–050°) in westerly locations and to the north to NW (0°–270°) in easterly locations. However, at two locations, measurements indicate south to SE (90°–195°) current directions (Fig. 5).

Along the NW margin of the basin very similar conglomerates unconformably overlie the Hatay ophiolite. At some localities the basal sediments are composed of pale, fine-grained, serpentinite-derived, indurated mudstone with scattered serpentinite clasts. Clast abundance increases upwards, passing into matrix-supported conglomerate, in turn overlain by a palaeosol (up to 25 m thick). This contrasts with the succession on the SE margin, where lenticular conglomerates are instead prominent. The thickness of the Lower Miocene succession on the NW margin varies from 0 to *c.* 175 m; in contrast, the succession reaches a maximum thickness of *c.* 300 m along the SE margin. On both margins the Lower Miocene succession thins and disappears towards the present coast.

The Lower Miocene succession is interpreted as a braided-river environment, in which sheet-flow processes dominated, forming the laterally continuous stratigraphically lower conglomerates. Higher in the formation, as observed in the SE, conglomerates are confined to channels, forming lenticular bodies; soils formed within inter-channel areas. A decrease in clast size upwards and the presence of foresets at the very top of the formation may indicate a decreasing palaeoslope with time. Palaeocurrent data, although variable, show that flow was generally to the north or west. The differences in palaeocurrent directions between the easterly and westerly exposures partly reflect a combination of

Table 1. *Age, lithology and microfossil data for the sediments of the Hatay Graben*

Formation Name	Age	Lithology	Selected Microfossils
Samandağ	Pliocene	Marl and sandstone	*Globerinoides ruber, Globorotalia scitula, Globigerinoides trilobus, sacculifer**
Vakıflı Member	Messinian		*Globoquadrina altispira*
Nurzeytin	Serravalian–Tortonian	Marl, limestone and sandstone	*Orbulina universa, Hastigerina rom.* sp., *Orbulina suturalis**
Sofular	Langhian	Limestone	*Praeorbulina gloerosa curva, Orbulina suturalis**
Balyatağı	Aquitanian–Burdigalian	Conglomerates and palaeosols	*Globergerinoides triobus, Globergerinoides ruber**
Kışlak	Lutetian	Limestone and marl	*Acarinina bullbrooki, Morozovella spirulosa**
Okçular	Lutetian	Limestone	*Morozovella aragonensis, Globigerina ineqispira**
Kaleboğazı	Late Cretaceous	Limestone and sandstone	*Globotruncana arca, Globotruncana gansseri, Globotruncana mayaroensis*†

*Şafak 1993*a*.
†Pişkin *et al.* 1986.

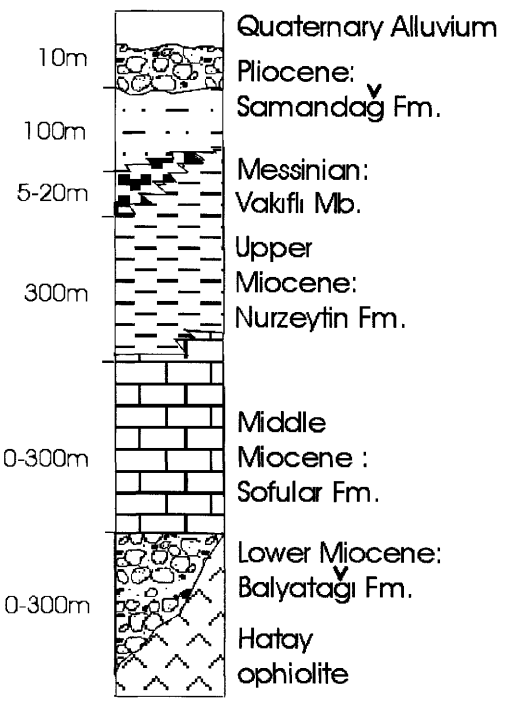

Fig. 3. Generalized stratigraphic column of the stratigraphic succession, not to scale.

regional and local palaeotopographic controls. The Hatay Graben was not clearly present in its current form, as braided rivers flowed northwards over an undissected topography, in contrast to the present flow through a dissected and faulted topography westwards into the Mediterranean Sea. The anomalous southerly flow data were recorded near the top of the formation and might record bypass of the basin and the inception of flow towards the present coast. The dominantly ophiolitic composition of the conglomerates suggests a source from ophiolites that were regionally emplaced southwards over the Arabian Platform during latest Cretaceous time (Yılmaz 1993; Robertson 2002). As the flow was dominantly northwards and westwards the main source was probably ophiolites located to the south or east of the Hatay Graben, as now exposed in the Kızıldağ Massif to the west and in the Baër-Bassit Massif to the SE, in Syria.

Middle Miocene (Sofular Formation; Fig. 3, Table 1)

The base of the Middle Miocene succession overlies Lower Miocene conglomerates in the north of the area on both sides of the graben. The basal contact is sharp with small, localized angular unconformities ($<5°$). Additionally, on the NW margin in the SW of the area these sediments overlie an eroded surface of the ophiolite (Fig. 4d). Along the NW margin the thickness of the succession increases from the NE to SW from 1–2 m to a maximum of *c.* 150 m. The basal Middle Miocene sediments are bioclastic limestone, generally wackestones, characterized by shallow-marine fauna including abundant bivalves, gastropods, corals and echinoids, together with oncolites, indicating low-energy conditions. In addition to bioclastic carbonates,

Fig. 4. (**a**) View to the east of the type section of the Balyatağı Formation (Lower Miocene) near the village of Enek; (**b**) thick turbiditic sand beds in marl (Nurzeytin Formation); car for scale; (**c**) dewatering pipe in alternating beds of hard and soft marly limestone with chert nodules, observed in the upper part of the Middle Miocene sequence at Çevlik; (**d**) Middle Miocene sediments overlying serpentinite along an irregular erosion surface. (Note the large gastropod in the top right corner; pen for scale, bottom right.)

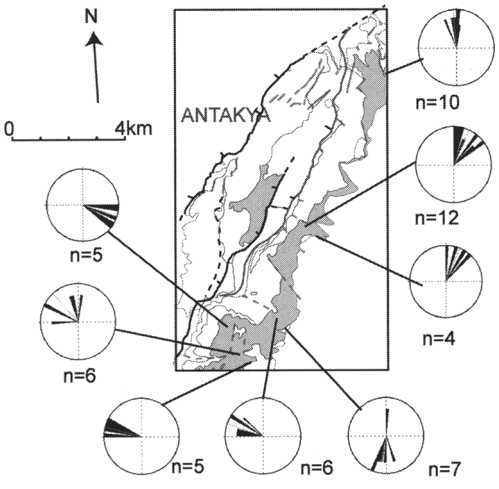

Fig. 5. Location map and rose diagrams showing the directions of palaeocurrent flow of the Lower Miocene conglomerates (Balyatğı Formation shaded in grey) along the SE margin of the basin. Box corresponds to the area shown in Figure 2.

sandstones with low-angle cross-bedding (indicating southward current flow), conglomerates and palaeosols are present near the base of the succession in the NW. The sediments exposed in coastal exposures on the NW margin are typically bioturbated, bioclastic calcirudites. Sedimentary structures are uncommon but parallel laminations and a dewatering structure (Fig. 4c) were observed locally. Along the SE margin of the basin, the succession thickens towards the south, to a maximum of *c.* 300 m and is similar to that seen on the NW margin. In the south, at Kozkalesi (Fig. 2), the lower part of the formation includes repeated palaeosol horizons with sharp bases, grading into bioclastic limestones (Fig. 6). The total thickness of these cycles exceeds 100 m. Upwards, palaeosol horizons gradually disappear and bioclastic calcirudites dominate the succession, rich in oncolites and reworked bioclastic material.

The Middle Miocene succession thins to the NE, as a result of greater subsidence in this area. The sharp base of this formation, without

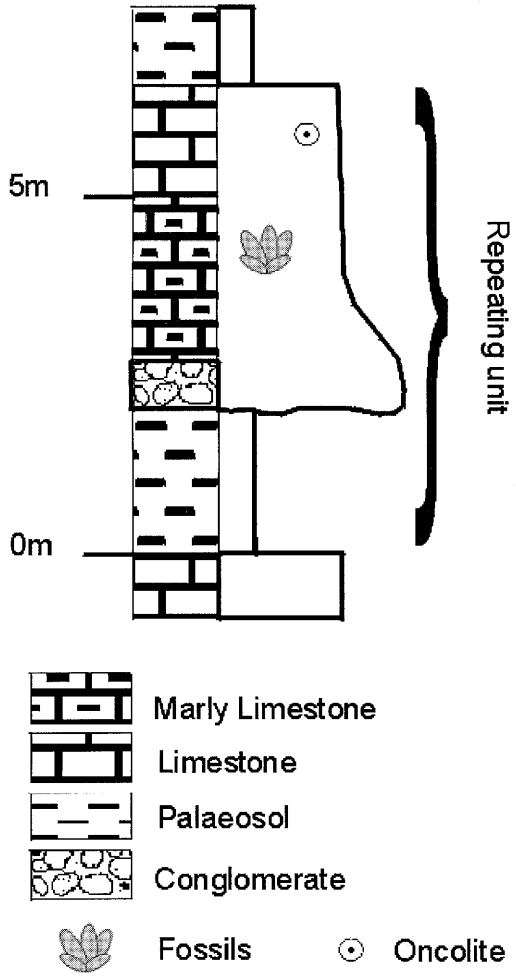

Fig. 6. Representative log showing the sedimentary cycles observed at Kozkalesi (Fig. 2).

erosional features, is suggestive of a rapid marine transgression. Local unconformities at the base of the formation suggest that the palaeotopography of the basal contact was irregular. Initially, water depths were very shallow (*c.* 0–10 m) along both basin margins, as there is evidence of coastal and non-marine processes (i.e. low-angle cross-bedding and soil formation), together with a coral build-up at one locality. The carbonates observed at Kozkalesi are interpreted as peritidal cyclothems on a carbonate platform. Sedimentation kept place with subsidence initially but the rate of subsidence apparently increased with time, resulting in deeper-water conditions possibly caused by tectonic subsidence; also there was an eustatic sea-level rise during this time (Haq *et al.* 1987). Planktic:benthic foraminiferal ratios (Meschede *et al.* 2002) suggest a water depth of <200 m for the upper part of the formation in this area. The thick succession on the NW basin margin shows evidence of sediment instability and gravity reworking (i.e. dewatering structures; slumps).

Late Miocene (Nurzeytin Formation; Fig. 3, Table 1)

The contact between the Middle and the Late Miocene successions is gradational, marked by 5–20 m of interbedded bioclastic limestone and marl. This contact is defined as the level at which marl exceeds bioclastic limestone. A thick (*c.* 300 m) marl sequence dominates the Upper Miocene succession and is exposed both within the present topographic graben and to the SE of the basin margin. The marl is a relatively uniform medium grey, very fine-grained, well sorted and contains a rich fauna of benthic Foraminifera (e.g. *Uvigerina peregrina*) and planktic Foraminifera (e.g. *Orbulina universa*), together with occasional bivalves. Planktic:benthic foraminiferal ratios suggest a water depth of up to 700 m (Meschede *et al.* 2002). White mica (muscovite) is not present in the lower part of the marl sequence; however, in more northerly exposures outside the Hatay Graben, near Belen (Fig. 1), and higher in the basin sequence as a whole the sediments become markedly micaceous. Numerous beds composed of mixed calcareous and terrigenous material are interbedded with the marl; these beds vary from 1–2 cm to >2 m thick. In the SW of the basin, calcarenite beds exhibit erosive bases with flute and groove casts, together with parallel and cross-lamination. Other calcarenites are massive, with bed thicknesses ranging from 0.1 to 2 m. In the same area a matrix-supported conglomerate horizon >5 m thick was observed. The matrix of this conglomerate is composed of grey marl with clasts of calcarenite and marl, up to 2–3 m in size. Further NE, interbeds are composed of medium- to coarse-grained litharenite, in beds 0.05–2 m thick (Fig. 4b). These beds are mostly massive, although parallel- and cross-lamination, ripples, flutes and mud rip-up clasts were locally observed. These structures yielded rare palaeocurrent directions; these are very variable (090°–300°) but generally are orientated towards the axis of the graben. On the SE flank of the basin (outside the modern topographic graben), there is a similar thickness of marl, but litharenite interbeds are absent.

The marl sequence is interpreted as background sedimentation in a relatively deep-water setting. The interbedded coarse sediments were probably reworked downslope as turbidites,

grain-flows and low-density debris-flows, reflecting instability of the basin margins. The lack of reworked material within the Upper Miocene succession outside the present basin suggests that at least some basin topography had developed by this time, causing sediment flows to bypass the relatively higher basin flanks and be deposited on the basin floor. The presence of muscovite in the stratigraphically higher sediments is interesting as there is little or no mica present in the basement rocks of the Hatay region; this suggests that this material is extrabasinal and was probably derived from the Tauride Mountains to the north.

Messinian (Vakıflı Member; Fig. 3, Table 1)

During the Messinian, the Mediterranean as a whole was affected by the Messinian salinity crisis (Hsü *et al.* 1978; Krijgsman *et al.* 1999). However, perhaps reflecting its marginal setting, only four evaporite localities are known in the Hatay Graben; three of these are near the axis of the modern graben and one on the SE margin (Fig. 2). The present altitude of gypsum ranges from 130 m above sea level (a.s.l.) near the graben axis to 320 m a.s.l. (Fig. 2) in the SE. The thickest gypsum deposit (25 m) is mainly composed of fine-grained alabastrine gypsum (location a; Fig. 2). The exposure includes large angular blocks (>2 m) of laminated alabastrine gypsum set in a gypsiferous marl matrix. In places, the alabastrine gypsum has undergone diagenetic alternation to coarse selenitic gypsum. Other sequences (5–10 m thick) comprise coarse-grained selenitic gypsum (locations b, c, d; Fig. 2). Exposures b and c consist of massive selenitic gypsum. It is not clear if this is primary or diagenetic. Location d, by contrast, consists of several exposures where a succession can be measured. The basal gypsum is made up of banded–stacked selenite (e.g. as reported from Cyprus; Robertson *et al.* 1995), with repeated layers of selenite crystals, 1–5 cm in size. The upper part of the sequence is composed of thick (>1 m), massive, fragmented selenite crystals, 5 cm or more in size, interpreted as debris-flow deposits.

The gypsum formed when the basin became semi-isolated from the Mediterranean Sea as a result of a falling sea level (Hsü *et al.* 1988). The fine-grained albastrine gypsum probably precipitated at the sediment–water and air–water interfaces (e.g. Schreiber *et al.* 1976). After precipitation, the gypsum was probably reworked into local depocentres, forming the banding seen at location d. The selenitic gypsum formed in a very shallow sub-aqueous marginal environment. We interpret the alabastrine gypsum (location a; Fig. 2) as material that was reworked towards local depocentres, in line with its present position near the axis of the modern graben. By contrast, the selenitic gypsum at locality d (Fig. 2) probably formed near the margin of the basin in a very shallow-water environment. The broken selenite crystals at the top of this succession possibly represent gypsum debris flows that were triggered by sea-level change or tectonic activity.

Pliocene (Samandağ Formation; Fig. 3, Table 1)

Pliocene sediments crop out only near the modern basin axis. Following the Messinian, a Pliocene transgression resulted in a return to marl deposition (Hsü *et al.* 1978). The marls resemble those of the underlying Upper Miocene succession but now contain a diverse shallow-marine fauna and common plant material. Within this marl sequence coarse siliciclastic horizons can be observed near the axis of the graben, for example, as thin (<5 cm), lenticular uncemented sand horizons (<1 m) with parallel lamination and rip-up clasts. There are also matrix-supported lenticular conglomerates, with subangular to rounded clasts (up to 1 m in size). Graded sand–mud horizons with erosive bases and tops can also be observed within the marl. Elsewhere, in the SW, Lower Pliocene sediments are composed of coarse-grained litharenite, rich in bivalves, often as discrete horizons, lacking sedimentary structures. Low-angle cross-bedding, ripples, parallel lamination and conglomerate lenses are present higher in the succession. Palaeocurrent directions are variable and show a range of directions from 060° to 225°. In contrast, the Upper Pliocene succession is generally composed of poorly cemented, coarse-grained, orange-weathering litharenites that are massive bedded and contain no bioclastic debris.

Following the Early Pliocene transgression, normal marine sedimentation resumed. The ratios of planktic:benthic Foraminifera (*c.* 0.9) suggest a water depth of <200 m. Background marl sedimentation was interrupted by the input of siliciclastic material by gravity processes. Exposures in the SW of the basin are typical of coastal deposits. Low-angle cross-bedding is associated with small gravel channel structures that are composed of rounded and sorted pebbles; these features are typical of beach processes. The succession probably represents sequence shallowing upwards from lower shore-face (sandy marl with bivalve lags) to upper shore-face and beach. By the end of the Pliocene, relative sea level had fallen further and the Hatay Graben became non-marine.

Quaternary alluvium (Fig. 3)

Quaternary sediments are composed of coarse sands, gravels and conglomerates. Sediments are preserved in four main river terraces that formed progressively as the Asi Nehir (Fig. 1) cut progressively downwards into the underlying strata, towards the present coastline. The coarse-grained sediments of these terraces are similar in composition to those of the modern river (mainly carbonate clasts and serpentinite), and are generally formed of subrounded to rounded clasts with little or no matrix. The sediments are usually massive bedded but large (2.5 m) high-angle cross-beds and erosional features are present in some exposures. In addition, Quaternary fault talus composed of poorly sorted, angular clasts and palaeosols was observed adjacent to major fault planes, especially to the south of Antakya. Also, around the town of Harbiye, tufa (cool-water carbonate) >50 m thick was locally precipitated from streams flowing down a high-angle fault scarp.

The Quaternary fluvial facies accumulated from a river system, characterized by meandering to braided channels, much as today. The progressively lower position of the terraces was caused by a relative sea-level fall, causing incision. Raised beaches, marine erosion notches and benches, and remnants of bioconstructed rims are found along, or near, the present coastline and these have been used to document two phases of rapid late Quaternary uplift (Pirazzoli *et al.* 1991).

Synsedimentary deformation

Synsedimentary structures can be used to determine the relative timing of faulting. Key features are growth faults, sediment packages thickening into normal faults (i.e. sediment fanning), intraformational faults and phases of fault motion, as inferred from fault-derived talus.

Synsedimentary features are absent from the Lower Miocene succession. However, three growth faults were identified within the Middle Miocene succession on the SE basin margin, near Kozkalesi (Fig. 2, location 1). Limestones are displaced by normal faults that dip northwestwards towards the axis of the basin and strike NE–SW. In two of these exposures there is a greater sediment thickness on the hanging-wall block compared with the footwall; undeformed strata overlie these faults (Fig. 7). In addition, within an upper Middle Miocene coastal exposure on the NW basin margin, beds at the base dip more steeply (35°) than those at the top (25°) as a result of sediment fanning (Fig. 2, location 2).

Sediment fanning was observed within Upper Miocene sediments at two localities elsewhere: one on the basin axis (Fig. 2, location 3) and one on the SE margin between two basin-bounding faults (Fig. 2, location 4). At the basin axis locality, the fanning (observed in a valley) was revealed by the difference in the angle of dip between the upper and lower beds (*c.* 10°). At location 4 (Figs 2 and 7), along the River Asi, the lower beds are subvertical, with the dip gradually decreasing upwards to *c.* 30°. These fanning sediments thicken towards the SE graben margin and it is possible that they thicken towards a graben-bounding normal fault.

Pliocene sandstones are highly deformed adjacent to major basin-bounding faults, with dips as high as to 90° locally (Fig. 2, location 5), implying that these faults are Pliocene or older. Microfaulting is commonly developed within axial Pliocene sediments; also, a growth fault and evidence of slumping were observed at location 6 (Fig. 2).

Several angular discordances were observed within a Quaternary talus cone adjacent to a major fault bounding the SE margin of the graben (near the village of Dursunlu; Fig. 2). It is inferred that the talus was derived from the adjacent exposed fault scarp; this fault then moved, rotating the pre-existing talus and producing more material that was deposited on top of the original sediment along a discontinuity (Fig. 2, location 7). This process was repeated, creating multiple small-scale discontinuities within the talus fan.

Only occasional faults were observed within the Quaternary deposits, probably because of the difficulty of recognition in such coarse and poorly consolidated sediments. However, rare faults were identified and locally the boundary between Pliocene sandstone and Quaternary conglomerate is faulted, confirming that fault motion has taken place during the Quaternary (Fig. 2, location 8).

The synsedimentary features described above suggest that growth faulting began in the Mid-Miocene. During the late Mid-Miocene and Late Miocene fault motion resulted in the tilting of bedding and the creation of accommodation space, creating the local sediment fanning. The present elevation of the Messinian evaporites (up to 320 m; Fig. 8) suggests that there has been significant post-Messinian fault uplift; evaporites on the basin margin are now 190 m higher in altitude than similar deposits near the basin axis. This, in turn, suggests that after the Messinian the basin underwent a phase of subvertical fault movement. Faulting additionally deformed the

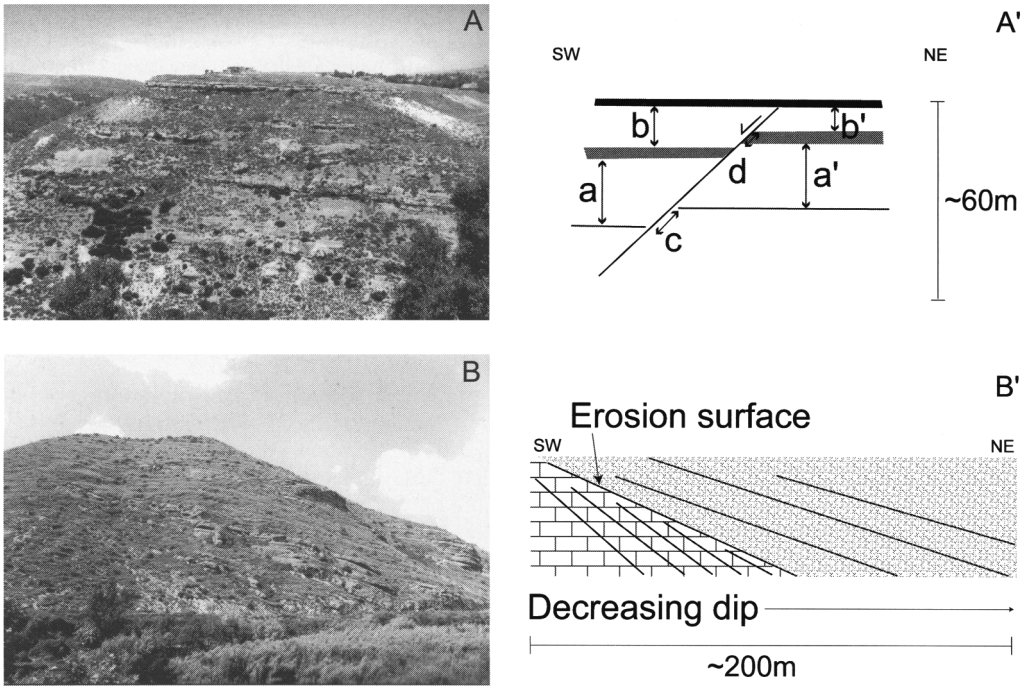

Fig. 7. (**a**) Photograph of a growth fault observed near the village of Kozkalesı in Middle Miocene limestone. (**b**) Sketch of the geometry of the fault. It should be noted that the lower intervals (a and a') are displaced by the fault but are of the same thickness. Upwards, interval b has a greater thickness than b'. The throw on the fault increases downwards. The upper package of strata is not cut by the fault. Therefore, the fault began moving after time A, and was moving during the deposition of b but had ceased moving when the upper layer was deposited. (**c**) Photograph showing the Middle Miocene fanning sediments exposed along the River Asi. (**d**) Sketch of the fanning sediments; it should be noted that the dip of the bedding decreases up section. In the middle of the section is a bored intraformation unconformity; below are fine limestones (mudstone) and above are dominantly bioclastic calcirudites with some conglomerate horizons.

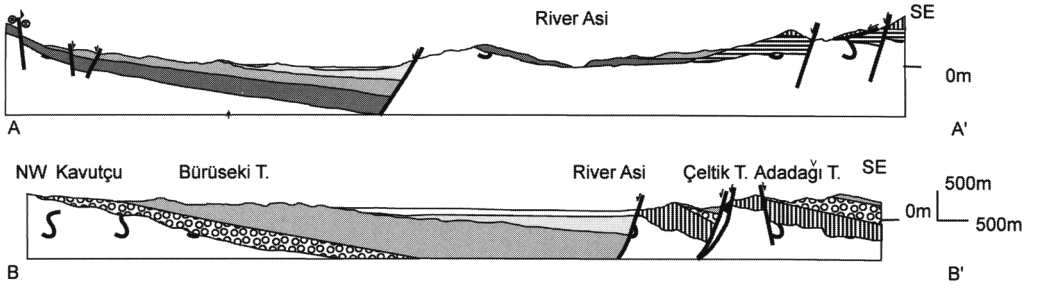

Fig. 8. Structural cross-sections of the Hatay Graben (see Fig. 2 for locations of sections and key).

Pliocene sediments and Quaternary talus throughout the basin. There is also the evidence of palaeoseismic to recent seismic activity from small earthquakes (US Geological Survey National Earthquake Information Centre). Within the past two centuries the city of Antakya has been devastated by large earthquakes, two notable events occurring on 13 August 1822, $M \approx 7.4$ and 13 April 1872, $M \approx 7.2$ (Över *et al.* 2002).

Structure of the Hatay Graben

The Hatay Graben is an asymmetrical structure (Fig. 8) trending 030°–210°. The SE margin is characterized by normal faults. A number of en echelon fault segments step away from the axis of the graben to the east, forming two arrays of subparallel faults (Fig. 2). The outer array comprises three main segments, whereas the inner array is shorter with two main fault segments. The greatest throw (>200 m) is on the innermost of the major faults. Small (<10 km²) sub-basins have formed on the margins of the graben as a result of the back-rotation of fault blocks. On the NW margin of the graben, map-scale faults (*c.* 100–200 m of displacement) dip into the graben; however, it appears that these are not as large as the faults bounding the SE margin.

In total, over 850 measurements were made of fault planes in the field area. When these data are considered together, the majority of the faults strike between 060° and 320°. Three main trends in the strike direction of large faults are recognized (Fig. 9): (1) NE–SW (*c.* 035°–060° to 215°–240°), parallel or subparallel to the basin margins; (2) NW–SE (*c.* 140°–160° to 320°–340°), orthogonal to the basin margins; (3) north–south (*c.* 350°–010° to 170°–190°), oblique to the basin margins. The majority of the faults trend either parallel to the graben or at a high angle to it (i.e. NW–SE). Normal, oblique, sinistral and dextral strike-slip faults are common, plus rare reverse faults. The direction of dip is variable, with the majority of faults being high angle.

To aid interpretation, the data were then divided into subgroups, first by structural domain (Fig. 9a) and then by the maximum age. The maximum age was determined from cross-cutting relationships, syndepositional structures and the age of displaced units in which the structures occur.

Cross-cutting relationships did not reveal any consistent trend, suggesting that there was only one identifiable phase of deformation. Two sets of slickenlines were observed on a few fault planes. Of these, one set of lineations on a fault plane is commonly oriented at a high angle (dip-slip) and the other at a low angle (oblique or strike-slip). However, it was not possible to confirm if one set of the two slickenlines was the younger, based on only a small number of measurements (n = 13).

When the faults are considered by geographical area (Fig. 9) the graben margins exhibit predominantly basin-parallel normal faults. However, there is also a significant number of faults trending at a high angle to the graben. For example, in zones 4 and 6 numerous faults trend east–west. The faults in zones 2 and 3, covering the axial zone of the graben, are less influenced by basin-parallel faults, although there is still a significant number of normal faults oriented in this direction. The main trends are north-south or NNW–SSE. These faults are predominantly extensional but there is also a significant number of strike-slip (sinistral and dextral) faults.

When fault patterns are considered according to the age of the formation in which they are observed, the patterns for each of the age categories, from Eocene to Pliocene, are very similar, with three main trends distinguishable (Fig. 10). Basin-parallel faults are not well represented within the Pliocene sediments, probably because Pliocene sediments are exposed only near the graben axis. The Pliocene also has greater numbers of strike-slip faults compared with other time periods. Faults within the Upper Cretaceous rocks exhibit a more north–south trend and may reflect a pre-existing stress regime. As there is little evidence that the normal and strike-slip faults in the Hatay Graben represent separate stages of faulting (of different age) we consider it likely that these variably trending faults coexisted in a transtensional setting.

Kinematics of faulting

A number of recent studies have investigated the process of oblique extension (transtension), both experimentally (Withjack & Jamieson 1986; Clifton *et al.* 2000; Tron & Brun 1991; McClay & White 1995) and using field evidence (Umhoefer & Stone 1996; ten Veen & Kleinspehn 2002). Transtension represents a range between two end-members: pure extension and strike-slip (where the trend of the basin is oblique to the extension direction). The acute angle, α, between the rift trend and the direction of displacement on the plate edge is inversely related to obliquity; thus, a largely oblique regime (i.e. strike-slip basin) exhibits a low value of α. In areas of pure extension ($\alpha = 90°$) the majority of the faults are normal and strike parallel or subparallel to the graben, with only small numbers of strike-slip faults accommodating changes in the amount of extension along strike; these faults strike at a high angle to the boundary faults. In contrast, in pure strike-slip regimes where $\alpha = 0°$ two dominant directions of faults occur *c.* 45° apart, and normal, reverse and strike-slip faults develop within the fault zone. Neither of these scenarios is applicable to the Hatay Graben, where three main directions of faulting were determined. One

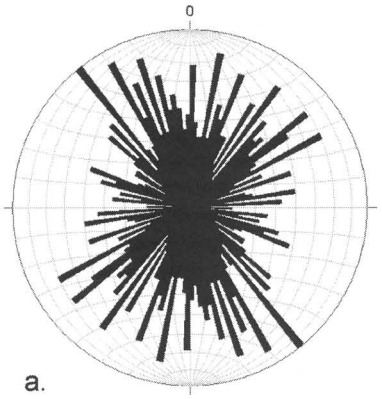

a.

2.5° classes

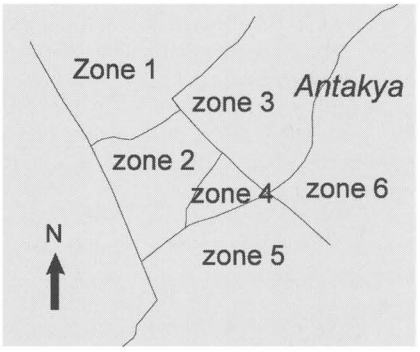

b.

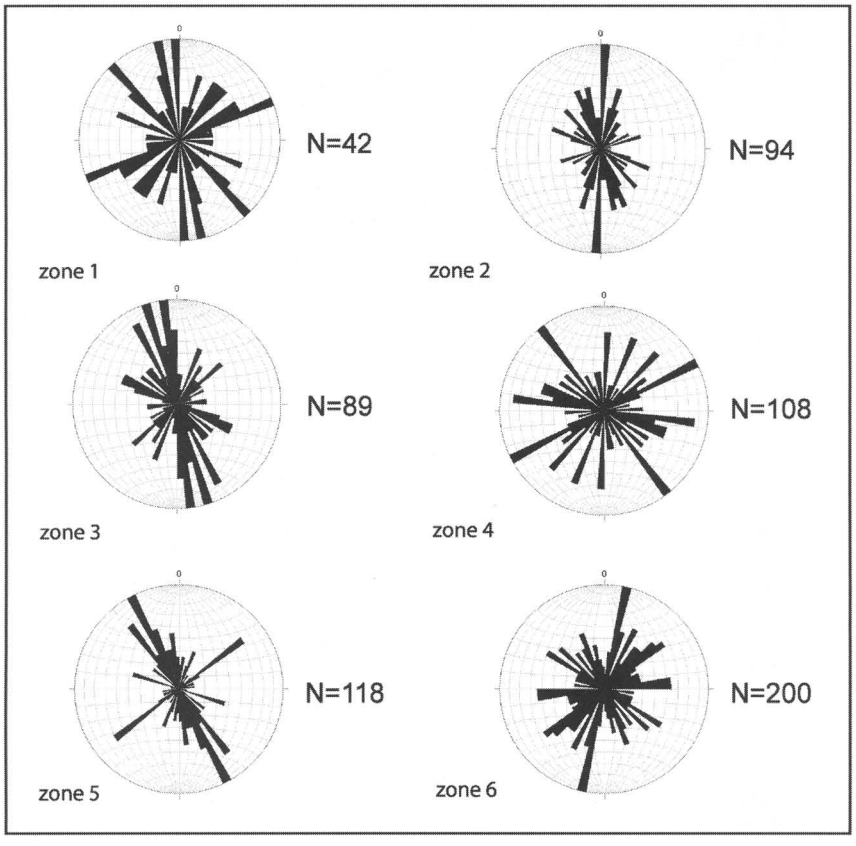

c.

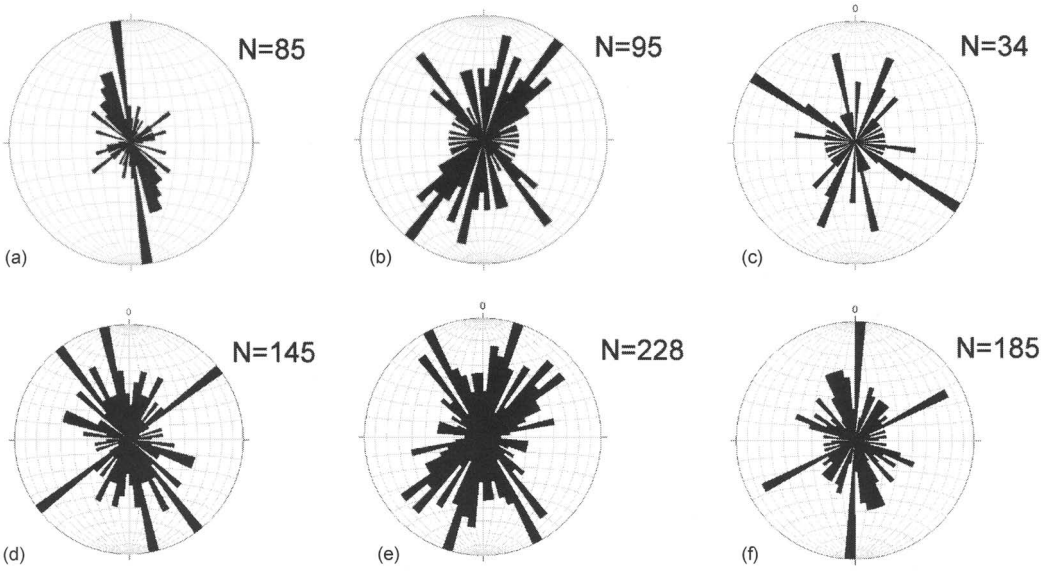

Fig. 10. Rose diagrams showing all of the structural data measured for the following periods: **(a)** Late Cretaceous; **(b)** Eocene; **(c)** Early Miocene; **(d)** Mid-Miocene; **(e)** Late Miocene; **(f)** Pliocene. Roses are divided into 5° classes.

$\alpha \leq 30°$, dip-slip, oblique-slip and strike-slip faults can develop in three populations. One population forms subparallel to the graben trend and two trend at a high angle to the rift and displacement direction. However, when $\alpha = 15°$ the majority of the faults are strike-slip in nature. We, therefore, infer that the deformation in the Hatay Graben reflects oblique extension at the present, where α is *c.* 30° (Fig. 11). A lack of strike-slip faults in older sediments suggests that the angle of extension has decreased over time and prior to the Plio-Quaternary α was perhaps $> 30°$.

To test this hypothesis and to gain a better understanding of the kinematics of faulting in the Hatay Graben, a stress inversion study was undertaken. This used the Angelier method (Angelier 1984), applied using the computer program Daisy 2.4 (Salvini 2001). The data were analysed using the same groups as before (i.e. age of formation and area). Figure 12 shows that zones 2 and 5 do not have a principal stress axis in the vertical and thus represent a transtensional stress regime. Zones 1, 3 and 6 have σ_1 positioned in the vertical; this is the maximum stress axis and relates to normal faulting. In these cases the minimum principal axis of stress, σ_3, is oriented NE–SW (188°, 033° and 210°, respectively) and normal faults are expected to trend NW–SE. In contrast, zone 4 has σ_2 in the vertical and therefore represents a strike-slip regime. When the fault data are considered by age (Fig. 13), the stress analysis results in σ_1 being vertical, thus corresponding to a normal palaeostress regime. The orientation of σ_3 is within the NE–SW quadrant of the stereonet.

This apparently anomalous result is likely to reflect the large number of NW–SE-oriented small faults from which slip data were obtained compared with the relatively small number of large bounding faults along which most of the fault motion took place; these are commonly weathered or slip data are rarely available owing in inaccessibility. Therefore, if more fault data could be collected a clearer result would be expected.

Evolution of the Hatay Graben

During latest Cretaceous–Eocene time, shallow-marine carbonates were deposited regionally across the Arabian platform. Sedimentary structures from the area studied indicate the presence of a slope dipping northwards towards the Neotethys Ocean. No sediments are known from Oligocene time, suggesting the area was then emergent and undergoing erosion. Eocene and older strata are folded indicating that fold and thrust tectonics caused uplift during this time; this was probably due to the southward migration of a flexural bulge related to continental collision along the Bitlis Suture to the north (Robertson *et al.* 2004).

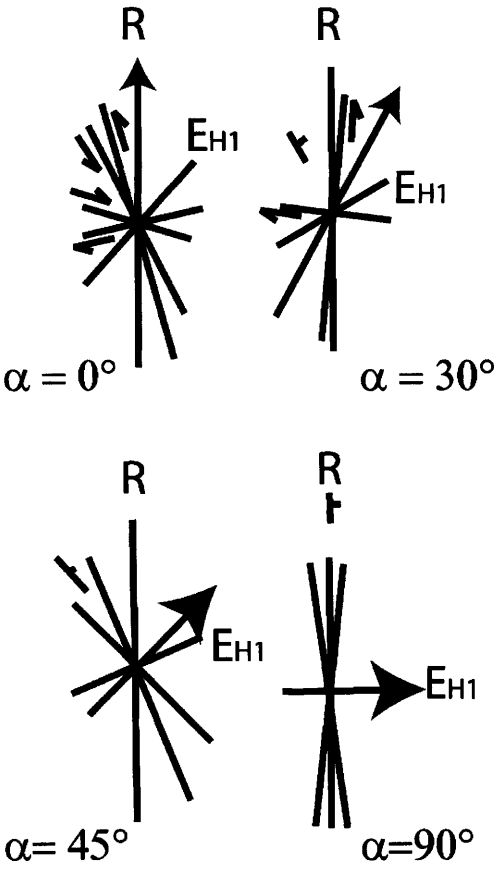

Fig. 11. Rose diagrams of fault trends predicted by a transtensional model (combined extension and sinistral shear). R is the rift trend; the large arrow indicates the direction of extension between the rift margins; E_{H1} is the direction maximum of extensional strain; modified from Withjack & Jamieson (1986).

At the beginning of the Early Miocene the Hatay area remained above sea level and large braided streams fed sediment across the eastern part of the basin, mainly from the south, depositing coarse conglomeratic units. These sediments were probably largely derived from the Baer–Bassit ophiolite massif, suggesting that uplift and unroofing of this area had occurred by this time. Some ophiolite-related sediment could also have been sourced from exposures now entirely eroded. The energy of the streams appears to have waned over time, possibly as the relief of the source area decreased. It is likely that the inferred flexural high remained during Early Miocene time, perhaps controlled by the inversion of the Neotethyan-age extensional faults in the basement.

The Mid-Miocene witnessed a marine transgression and shallow-marine bioclastic limestone deposition in a variety of subenvironments. Greatest thicknesses in the SW imply more accommodation space in this area, in turn suggesting that extension increased in this direction. The inferred growth fault and sediment fanning confirm that normal faults were active during Mid-Miocene time. These were oriented NE–SW, implying that σ_1 was vertical and σ_3 oriented *c.* NW–SE. By the Late Miocene, a rise in relative sea level led to moderately deep-marine conditions, and sufficient bathymetry to promote basin margin instability. The Mediterranean-wide salinity crisis during the Messinian resulted in the precipitation of evaporites, now exposed in only a few areas near the present basin axis and on its southern flank. Rapid uplift of the graben flanks took place during the Early Pliocene, displacing the evaporite horizon and confining Pliocene sediment deposition to within the present graben. The probable cause was a strong pulse of rifting with corresponding flexural uplift of the basin margins and relative deepening of the basin axis. Although marine sedimentation resumed in the Early Pliocene, relative sea-level fall culminated in continental conditions by the Late Pliocene, during a time when active faulting appears to have continued. During the Quaternary, continuing uplift has accentuated channel incision and formed wind-gaps, as seen on the SE margin. A series of river terraces formed inland and marine terraces developed (Pirazzoli *et al.* 1991) near the coast, reflecting continuing uplift during a time of global sea-level change. Historical seismicity (Över *et al.* 2002), and present-day seismicity, confirm that the area remains tectonically active at present, with normal and oblique faulting taking place (Över *et al.* 2002).

Regional comparisons and implications

The Hatay Graben can usefully be compared with the tectonic evolution of the Tauride Mountains to the NE and Cyprus to the west.

During the Cretaceous to Neogene, collisional processes affected the Taurus Mountains to the north of the Hatay Graben. The segment of the Bitlis suture directly north of the study area is the Misis–Andırın lineament (Robertson *et al.* 2004; Fig. 1). Ophiolites were emplaced southwards onto the Arabian foreland during the partial closure of the southern Neotethys Ocean in latest Cretaceous time. This ocean remained partly open during the Early Tertiary until final closure by Mid-Miocene time along the Bitlis suture, which runs through southern Turkey to

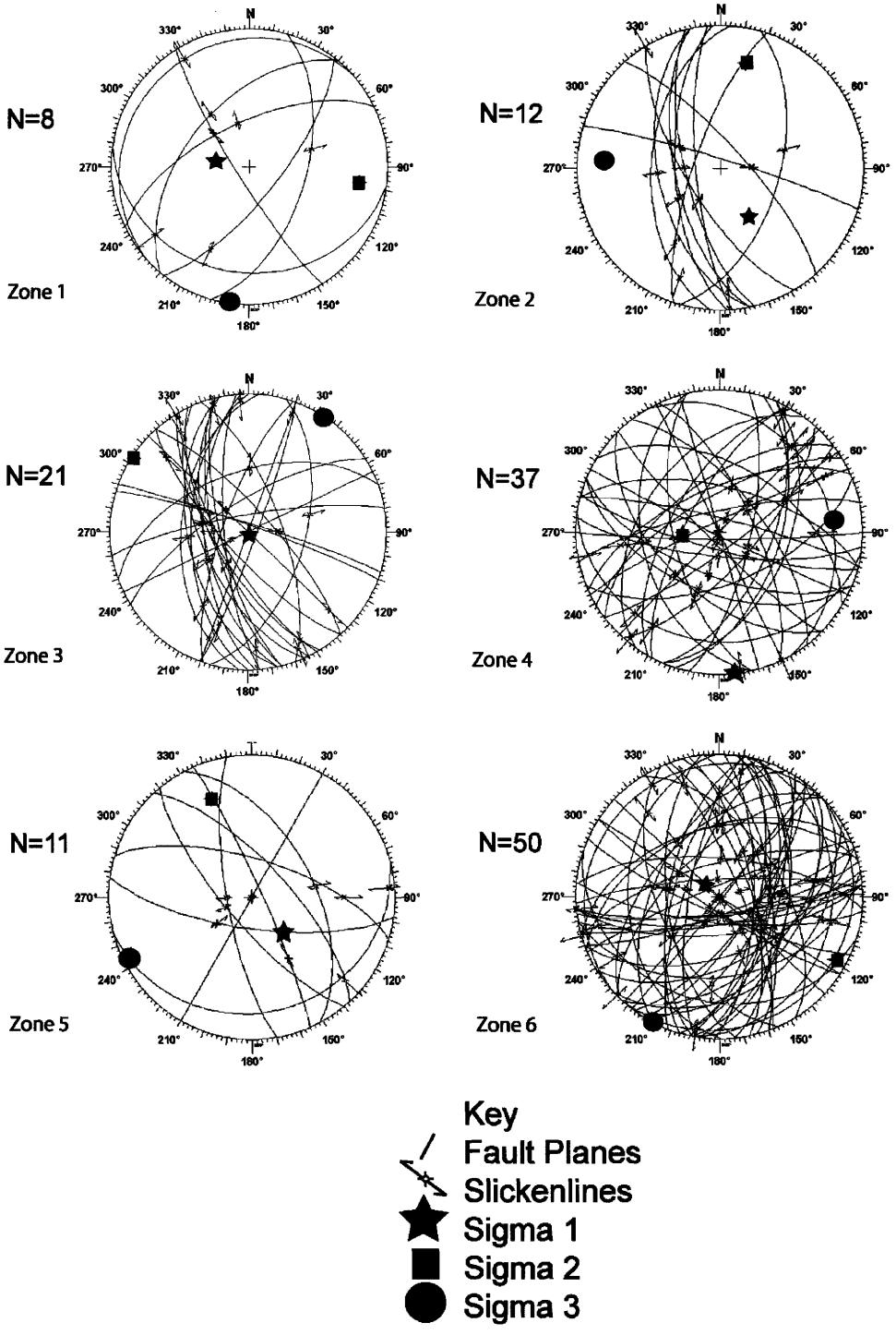

Fig. 12. Equal-area stereonets showing the results of the Angelier-method stress inversion where the data are divided by sub-area (see Fig. 9 for location of the zones).

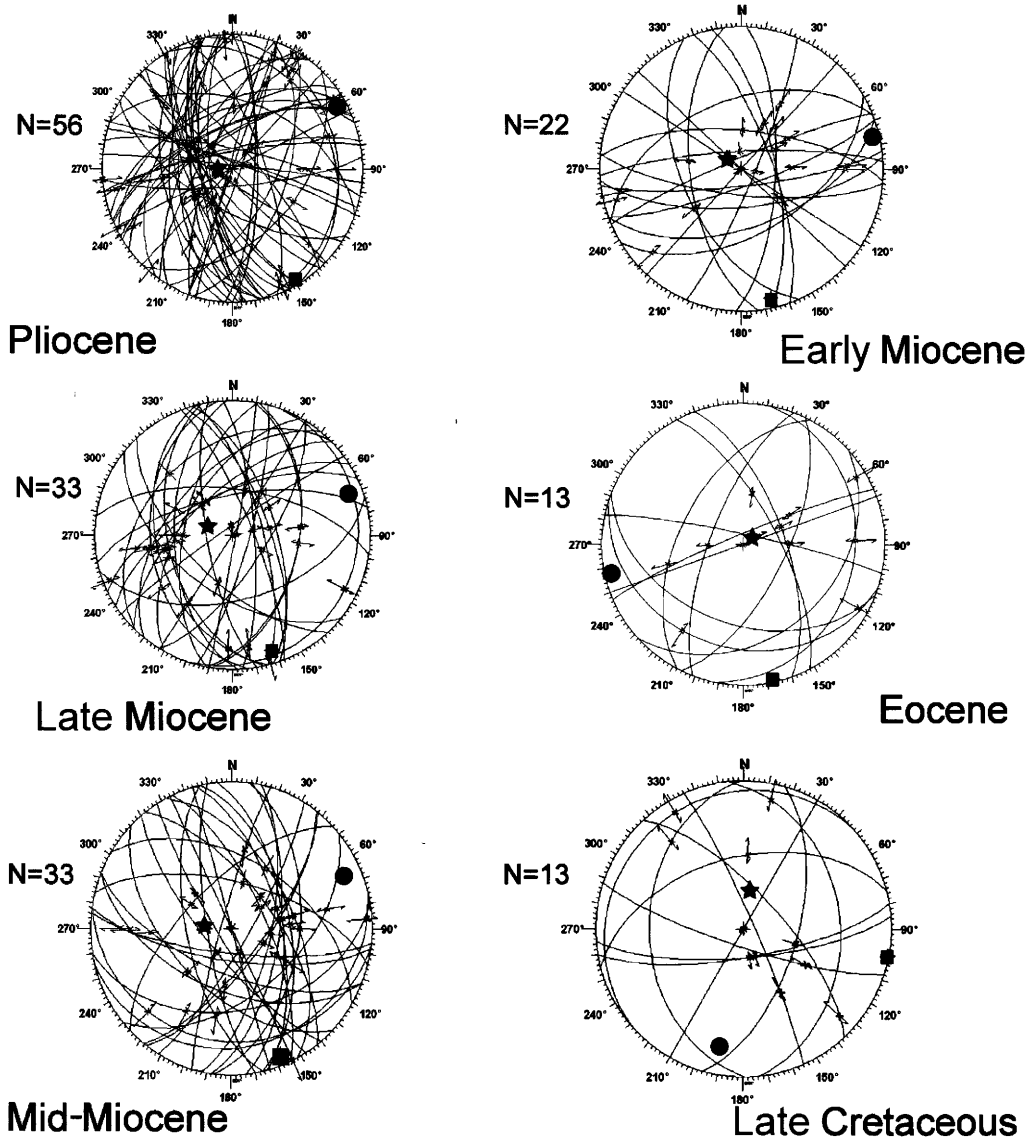

Fig. 13. Lower hemisphere equal-area projection of the results of the Angelier-method stress analysis when the data are divided by the minimum age of the fault (see Fig. 12 for key).

Iran (Dewey *et al.* 1986; Yılmaz 1993; Robertson 1998*a*).

After ophiolite obduction in latest Cretaceous time, passive margin conditions were restored along the northern margin of the Arabian plate, including the study area. By contrast, the northern margin of the southern Neotethyan ocean was characterized by northward subduction and active margin processes (Yılmaz 1993; Robertson 1998*a*). After a period of extension on the northern active margin during Mid–Eocene time, remaining Neotethyan ocean crust was subducted until diachronous continental collision was initiated. As the northerly Tauride active margin impinged on the Arabian passive margin, this was flexurally upwarped during the Oligocene and then collapsed to form a foreland basin during the Early to Mid–Miocene (e.g. Lice Formation in SE Turkey). Collision was complete by the Mid-Miocene, the earliest time when

transgression of the suture is observed. During the Mid–Late Miocene suture tightening took place until little further orthogonal shortening could take place (Robertson 2004). During Mid–Late Miocene time large volumes of clastic material were shed from the uplifting Taurus Mountains to the north, coupled with a much smaller amount of sediment sourced from the erosion of the inferred flexural forebulge to the south (Robertson *et al.* 2004). During the Early Pliocene there was then a switch to left-lateral strike-slip as the EAFZ became established (Şengör *et al.* 1985; Dewey *et al.* 1986; Hempton 1987; Westaway & Arger 1996). As a result, compressional strain was released across the foreland as a whole.

Miocene sediments directly to the north of the Hatay Graben are buried beneath the Iskenderun Basin. In general, exploration oil wells in this basin indicate that Upper Oligocene to Lower Miocene turbidites overlie ophiolitic rocks (Kempler & Garfunkel 1991), which were then covered by Messinian evaporites and Plio-Quaternary clastic sediments, prograding from the Misis–Andırın thrust front to the north (Aksu *et al.* 1992). On land, the Iskenderun Basin is marked by extensional faulting, especially around the northern margin of the Hatay ophiolite (unpublished data), opening a basin that was partially infilled with shallow-marine clastic sediments. Further north, thrust Miocene sediments structurally underlie the Misis Lineament, the southern front of the Tauride allochthon, and include Lower–Middle Miocene deep-water turbidites and Upper Miocene–Pliocene shallow-water clastic deposits (Gökçen *et al.* 1988).

Cyprus is situated to the SW of the Hatay Graben. The Troodos Ophiolite formed in an above-subduction zone setting in Late Cretaceous time, in common with the chain of ophiolites that stretches from Cyprus, to Hatay, through SE Turkey and Iran to Oman (e.g. Robertson 2004). During the Miocene the present subduction zone, which dips NE under Cyprus (Pilidou *et al.* 2004), is likely to have been active. Subsequent rollback of this subduction zone resulted in extensional faulting during the Miocene, forming a number of basins in the area (e.g. Polis Graben, western Cyprus; Payne & Robertson 1995). The collision of the Eratosthenes Seamount with the Cyprus trench triggered the uplift of the Troodos Massif and the Kyrenia Range of northern Cyprus (e.g. Robertson 1998b) mainly during Late Pliocene to Pleistocene time. The Kyrenia Range continues offshore to connect with the Misis–Andırın lineament (Fig. 1) and can be considered as part of the original northern continental margin of the Southern Neotethys Ocean. Further south, the Latakia Ridge runs from southern Cyprus to northern Syria, coming onshore to the north of Latakia (Kempler & Garfunkel 1991; Ben-Avraham *et al.* 1995). Between these lineaments is the Latakia Basin, which may extend into the Mesaoria Basin on Cyprus. As such, the Hatay Graben is located at the interface between an area further to the east where continental collision took place by Mid-Miocene time followed by left-lateral tectonic escape, and an area to the west that is in a syncollisional setting with a deep-water basin still present. We consider that this particular setting has contributed to the tectonic development of the Hatay Graben.

Discussion

Three models can be considered to explain the tectonic evolution of the Hatay Graben; of these, model 1 is the only one previously considered in the literature.

Model 1: strike-slip related model

Basin formation took place in response to stresses caused by the propagation of the EAFZ, the DSFZ, or both. Some workers see the Hatay Graben as a direct extension of the EAFZ (Şengör *et al.* 1985; Lyberis *et al.* 1992; Şaroğlu *et al.* 1992), whereas others (Arpat & Şaroğlu 1972; Parlak *et al.* 1998) trace the DSFZ further north through the Amanos Mountains to the Turkish coast. Evidence from syndepositional faulting within the Hatay Graben indicates that normal faulting parallel to the present graben was taking place during the Mid-Miocene, around 13–15 Ma. However, the inception of the EAFZ is dated as Late Miocene to Pliocene (Şengör *et al.* 1985; Dewey *et al.* 1986; Hempton 1987; Şaroğlu *et al.* 1992; Westaway & Arger 1996; Yürür & Chorowicz 1998). In addition, the DSFZ formed synchronously with the opening of the Red Sea around 18–20 Ma (Garfunkel 1981; Hempton 1987; Lyberis 1988; Rojay *et al.* 2001). Studies of the northerly DSFZ indicate that the fault did not propagate northwards into northern Syria and southern Turkey for another 15 Ma, until a second phase of fault motion around 4.5 Ma (Freund *et al.* 1968; Girdler & Styles 1978; Zanchi *et al.* 2002). Therefore, the initiation of faulting within the Hatay Graben cannot be linked directly with the inception of either the EAFZ or the DSFZ, as the initiation of normal faulting predates the presence of the EAFZ and DSFZ in southern Turkey by *c.* 10 Ma. However, the inferred Plio-Quaternary

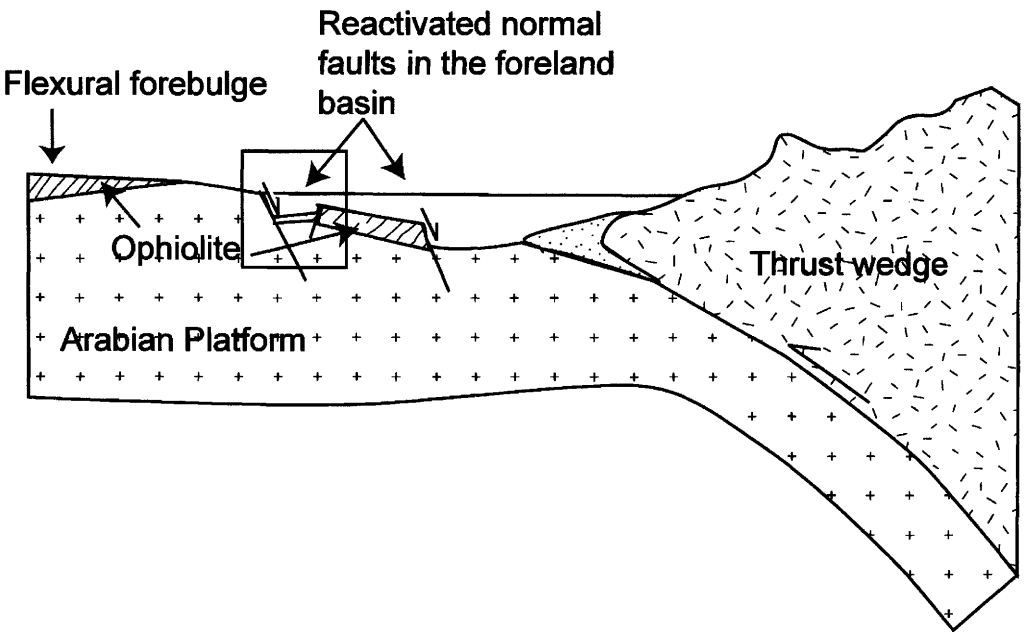

Fig. 14. Schematic diagram illustrating the model of basin formation with normal faulting occurring in the foreland basin. Box indicates location of the Hatay Graben.

transtension and related strike-slip faulting could be related to the EAFZ or DSFZ (see below).

Model 2: extension related to subduction roll-back

During the Early Miocene the Southern Neotethys to the north of the study area was in its final stages of subduction and incipient collision with the Arabian plate. The initiation of the graben, situated on the subducting Arabian slab, might relate to stresses associated with subduction, e.g. trench rollback caused by the negative buoyancy of subducting oceanic lithospheric crust. There is evidence that the overriding Tauride plate was strongly extended during the Early–Mid-Miocene, with the formation of thrust-top (piggyback) basins within the Misis–Andırın lineament to the north (Robertson *et al.* 2004). This extension could be related to rollback of the downgoing slab during the final stages of subduction when old, dense oceanic crust was being subducted. This model was proposed for several basins in the eastern Mediterranean (i.e. Polis Graben, Cyprus, Payne & Robertson 1995; Mesaoria Basin, Cyprus, McCallum & Robertson 1990; Robertson *et al.* 1991). However, these basins are situated on the overriding place of the subduction zone, not the foreland like the Hatay Graben, which is less likely to be affected by extension-related rollback.

Model 3: foreland basin followed by 'tectonic escape' model (Figs 14 and 15)

In this model the basin was initially part of the fill of a foreland basin developed ahead of the advancing Tauride allochthon. Peripheral foreland basins develop in response to loading of the lithosphere of the downgoing plate during continent–continent collision (Stockmal *et al.* 1986; Sinclair 1997). We believe that there was no distinct topographic graben present until Late Miocene–Pliocene time and that before this time the Hatay Graben area formed part of the foreland basin to the Bitlis Suture Zone. Models of continental collision suggest that the position of a flexural forebulge can be *c.* 400 km from the thrust front, making this feasible.

Normal faulting, as seen in the area studied, has been documented in many foreland basins; for example, the Taconic foreland basin (Utica Shale) of New York (Bradley & Kidd 1991), the Timor Trough (Veevers *et al.* 1978), the French Alps (Sinclair 1997) and the central Mediterranean, Pelagian Shelf (Argnani & Torelli 2001). Such normal faulting can be related to two factors. First, the underlying passive margin is likely

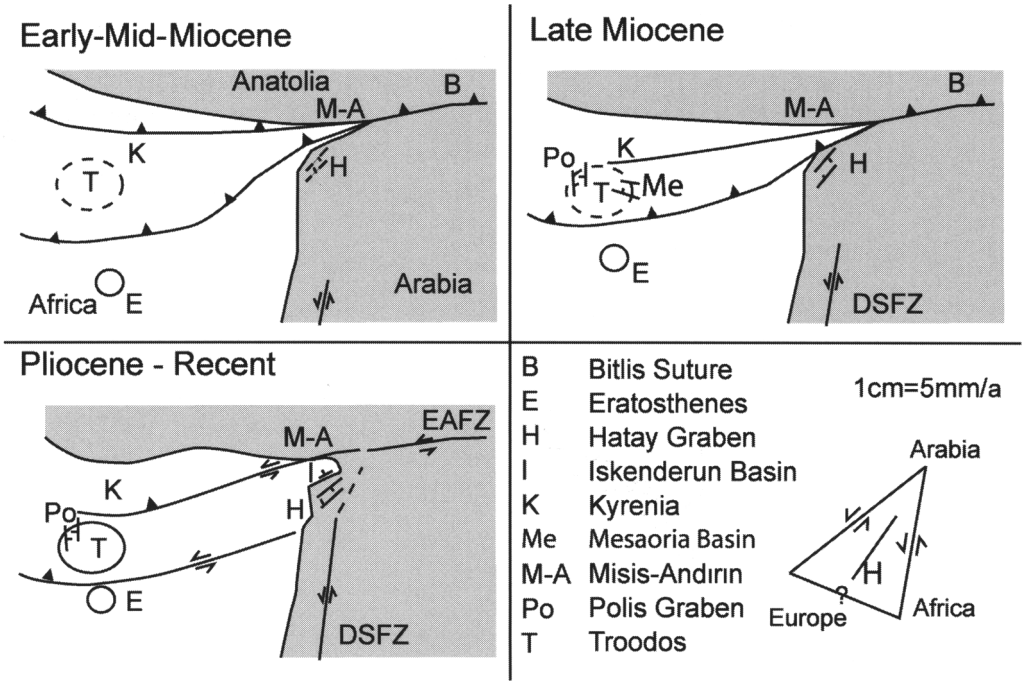

Fig. 15. Tectonic sketches illustrating the evolution of the Eastern Mediterranean from the Early–Mid-Miocene to the present day. The Early–Mid-Miocene is a time of subduction near the coast of Anatolia, subsequently migrating to the south. Thrusting occurs along the Arabian margin, forming a foreland basin. Faulting is initiated in the Hatay Graben. By the Late Miocene, 'rollback' of the subduction zone has given rise to extensional basins on the overriding plate and thrust emplacement is complete in southern Turkey. The DSFZ is propagating northwards. During Pliocene–Recent time, collision results in westward escape of Anatolia, initiating the EAFZ, and the DSFZ has propagated northwards into Southern Turkey. The Eratosthenes Seamount is being thrust under Cyprus, and the Troodos Massif is uplifting in response. The vector diagram illustrates the orientation and motion of the DSFZ and EAFZ, with the orientation of the Hatay Graben shown between them.

to have normal faults present that formed during continental break-up, forming deep-seated weaknesses in the lithosphere that could be reactivated later. Second, active faulting in the foreland may be due to extensional stresses generated on the outer arc of the fixed lithosphere (Bradley & Kidd 1991). However, it is more likely to have affected more proximal areas of the foreland basin than is represented by the Hatay Graben area. We, therefore, we suggest that the initiation of the Hatay Graben was due to extensional stresses caused by the flexure of the foreland that reactivated deep-seated normal faults in the Arabian passive margin.

A thick upper turbiditic 'flysch' sequence is not present, as in a fully developed foreland basin (e.g. Sinclair 1997), probably because by the Mid-Miocene southward convergence of the Eurasian and African (Arabian) plates in SE Turkey was replaced by left-lateral strike-slip and tectonic escape of Anatolia towards the Aegean. As a result, loading of the foreland diminished and thus allowed isostatic rebound and the observed regional regression to take place. We suggest the Plio-Quaternary deformation was transtensional because the Hatay Graben is located at the interface between a zone of continent–continent collision in the east and a syn-collisional zone in the west into which tectonic escape could take place.

Conclusions

The first evidence of a discrete basin in the Hatay area is from the Mid-Miocene time. Initial normal faulting was coincident with the basin becoming shallow marine in character. The basin progressively deepened during the Mid–Late Miocene, when deeper marine carbonate deposition dominated. During the Early Pliocene strong flank uplift and relative sea-level fall resulted in marginal-marine conditions followed by

non-marine conditions from Late Pliocene time onwards. There are three main trends of faulting (NW–SE, north–south, NE–SW). The fault patterns are dissimilar to those known from pure strike-slip or extensional settings but are similar to those recorded in oblique extensional (transtensional) settings (e.g. Gulf of California, Gulf of Aden). Fault stress analysis indicates that $\alpha = 30°–45°$ within a left-lateral (sinistral) shear zone (where α is the acute angle between the rift trend and the direction of displacement on the plate edge). The orientation of the graben was probably influenced by pre-existing zones of crustal weakness, probably including those of the Early Mesozoic rifting of Neotethys. Sediments of Late Miocene and younger age reflect the location of the developing basin near the distal edge of a foreland basin. During the Plio-Quaternary, when the present topographic graben developed, the main regional tectonic controls were the east-west left-lateral tectonic escape of Anatolia westwards along the East Anatolia Fault Zone and the northwards propagation of the DSFZ.

SJB acknowledges receipt of an NERC PhD Studentship (NER/S/A/2002/10361) and additional funding by the American Association of Petroleum Geologists. AHFR thanks the Carnegie Trust for financial assistance with fieldwork. We thank M. C. Alçiçek, N. Jaffey and M. Purvis, whose reviews improved this paper.

References

AKSU, A. E, ULUG, A. PIPER, D. J. W., KONUK, Y. T. & TURGUT, S. 1992. Quaternary sedimentary history of Adana, Cilicia and İskenderun Basins: northeast Mediterranean Sea. *Marine Geology*, **104**, 55–71.

ANGELIER, J. 1984. Tectonic analysis of fault slip data sets. *Journal of Geophysical Research*, **89**, 5835–5848.

ARGANI, A. & TORELLI, L. 2001. The Pelagian Shelf and its graben system (Italy/Tunisia). *In*: ZIEGLER, P. A., CAVAZZA, W., ROBERTSON, A. H. F. & CRASQUI-SOLEAU. S. (eds) *Peri-Tethys Memoir 6: Peri-Tethys Rift/Wrench Basins and Passive Margins*. Mémoires du Muséum National d'Histoire Naturelle, **186**, 529–544.

ARPAT, E. & ŞAROĞLU, F. 1972. The East Anatolian Fault System; thoughts on its development. *Bulletin of the Mineral Research and Exploration Institute of Turkey*, **78**, 33–39.

BARKA, A. A., AKYÜZ, S. H., COHEN, H. A. & WATCHORN, F. 2000. Tectonic evolution of the Niksar and Tasova–Erba pull-apart basins, North Anatolian fault zone: their significance for the motion of the Anatolian block. *Tectonophysics*, **322**, 243–264.

BEN-AVRAHAM, Z., TIBOR, G., LIMINOV, A. F., LEYBOV, M. B., IVANOV, M. K., TOKAREV, M. Y. & WOODSIDE, J. M. 1995. Structure and tectonics of the Eastern Cyprean Arc. *Marine Petrology and Geology*, **12**, 263–271.

BEYDOUN, Z. 1999. Evolution and development of the Levant (Dead Sea Rift) Transform system: a historical–chronological view of structural controversy. *In*: MACNIOCAILL, C. & RYAN, P. D. (eds) *Continental Tectonics*. Geological Society, London, Special Publications, **164**, 239–255

BOZKURT, E. 2001. Neotectonics of Turkey—a synthesis. *Geodinamica Acta*, **14**, 3–30.

BRADLEY, D. C. & KIDD, W. S. F. 1991. Flexural extension of the upper continental crust in collisional foredeeps. *Geological Society of America Bulletin*, **103**, 1416–1438.

BREW, G., LUPA, J., BRAZANGI, M., SAWAF, T., AL-IMAM, A. & ZAZA, T. 2001. Structure and tectonic development of the Ghab basin and the Dead Sea fault system, Syria. *Journal of the Geological Society, London*, **158**, 665–674.

CHAIMOV, T., BARAZANGI, D., AL-SAAD, D., SAWAF, T. & GEBREN, A. 1990. Crustal shortening in the Palmyride Fold Belt, Syria, and implications for movement along the Dead Sea Fault System. *Tectonics*, **9**(6), 1369–1386.

CLIFTON, A. E., SCHLISCHE, R. W., WITHJACK, M. O. & ACKERMANN, R. V. 2000. Influence of rift obliquity on fault-population systematics: results of experimental clay models. *Journal of Structural Geology*, **22**, 1491–1509.

DELALOYE, M., PISKIN, Ö., SELÇUK, H., VUAGNAT, M. & WAGNER, J.-J. 1980. Geological section through the Hatay ophiolite along the Mediterranean coast, southern Turkey. *Ofiliti*, **5**(2/3), 205–216.

DERMAN, A. S., AKDAĞ, K., GÜL, M. A. & YENIAY, G. 1996. Relationship between sedimentation and tectonics in the Maraş Miocene basin. *Turkish Association of Petroleum Geologists, 11th Petroleum Congress, Turkey*, 91–102.

DEWEY, J. F., HEMPTON, M. R., KIDD, W. S. F., ŞAROĞLU, F. & ŞENGÖR, A. M. C. 1986. Shortening of continental lithosphere: the neotectonics of eastern Anatolia—a young collision zone. *In*: COWARD, M. O. & REIS, A. C. (eds) *Collisional Tectonics*. Geological Society, Londons, Special Publications, **19**, 3–36.

FREUND, R., ZAK, I. & GARFUNKEL, Z. 1968. On the age and rate of sinistral movement along the Dead Sea rift. *Nature*, **220**, 253–255.

GARFUNKEL, Z. 1981. Internal structure of the Dead Sea leaky transform (rift) in relation to plate kinematics. *Tectonophysics*, **80**, 81–108.

GIRDLER, R. W. & STYLES, P. 1978. Seafloor spreading in the western Gulf of Aden. *Nature*, **271**, 615–617.

GÖKÇEN, S. L., KELLING, G., GÖKÇEN, N. & FLOYD, P. A. 1988. Sedimentology of a Late Cenozoic collisional sequence: the Misis Complex, Adana, southern Turkey. *Sedimentary Geology*, **59**, 205–235.

HAQ, B. U., HARDENBOL, J. & VAIL, P. R. 1987. Chronology of fluctuating sea-levels since the Triassic. *Science*, **4793**, 1156–1167.

HEMPTON, M. R. 1987. Constraints on Arabian Plate motion and extensional history of the Red Sea. *Tectonics*, **6**, 687–705.

HSÜ, K. J., MONDADERT, L., BERNOULLI, D., *et al.* 1978. History of the Mediterranean salinity crisis. *In*: HSÜ, K., MONTADERT, L. *et al.* (eds) *Initial Reports of the Deep Sea Drilling Project, 42*. US

Government Printing Office, Washington, DC, 1053–1078.

JAFFEY, N. & ROBERTSON, A. H. F. 2001. New sedimentological and structural data from the Ecemiş Fault Zone, southern Turkey: implications for its timing and offset and the Cenozoic tectonic escape of Anatolia. *Journal of the Geological Society, London*, **158**, 367–378.

KEMPLER, D. & GARFUNKEL, Z. 1991. The northeast Mediterranean triple junction from a plate kinematic point of view. *Bulletin, Technical University of Istanbul*, **44**(3–4), 425–454.

KOÇYIĞIT, A. & BEYHAN, A. 1998. A new intracontinental transcurrent structure: the Central Anatolian Fault Zone, Turkey. *Tectonophysics*, **284**, 317–336.

KRIJGSMAN, W., WILSON, D. S., HILGEN, F. J., RAFFI, I. & SIERRO, F. J. 1999. Chronology, causes and progression of the Messinian salinity crisis. *Nature*, **400**(6745), 652–655.

LOVELOCK, P. E. R. 1984. A review of the tectonics of the northern Middle East region. *Geological Magazine*, **121**, 577–587.

LYBERIS, N. 1988. Tectonic evolution of the Gulf of Suez and the Gulf of Aqaba. *Tectonophysics*, **153** (1–4), 209–220.

LYBERIS, N., YÜRÜR, T., CHOROWITCZ, J., KASAPOĞLU, E. & GÜNDOĞU, N. 1992. The East Anatolian fault: an oblique collisional belt. *Tectonophysics*, **204**, 1–15.

MART, Y. & RABINOWITZ, P. D. 1986. The northern Red Sea and Dead Sea rift. *Tectonophysics*, **124**, 85–113.

MCCALLUM, J. E. & ROBERTSON, A. H. F. 1990. Pulsed uplift of the Troodos Massif—evidence from the Plio-Pleistocene Mesaoria Basin. *In*: MALPAS, J., MOORES, E. M., PANAYIOTOU, A. & XENPHONTOS, C. (eds) *Ophiolites, Ocean Crustal Analogues. Proceedings of the Symposium 'Trodoos 1987'*. Geological Survey Department, Nicosia, 217–229.

MCCLAY, K. R. & WHITE, M. J. 1995. Analogue modelling of orthogonal and oblique rifting. *Marine and Petroleum Geology*, **12**, 147–151.

MCKENZIE, D. P. 1978. Active tectonism in the Alpine–Himalayan belt: the Aegean Sea and the surrounding regions (tectonics of the Aegean region). *Geophysical Journal of the Royal Astronomical Society*, **55**, 217–254.

MESCHEDE, M., WEISS, R., SCHMIEDL, G. & HEMLEBEN, C. 2002. Benthic foraminifera distribution and sedimentary structures suggest tectonic erosion at the Costa Rica convergent plate margin. *Terra Nova*, **14**(5), 388–396.

ORAL, M. B., REILINGER, R. E., TOKSÖZ, M. N., KONG, R. W., BARKA, A. A., KINIK, I. & KENK, O. 1995. Global positioning system offers evidence of plate motions in eastern Mediterranean. *EOS Transactions*, American Geophysical Union, **76** (9), 9–11.

ÖVER, S., KAVAK, K. Ş., BELLIER, O. & ÖZDEN, S. 2004. Is the Amik Basin SE Turkey a triple junction area? Analyses of SPOT XS imagery and seismicity. *International Journal of Remote Sensing*, **25**(19), 3857–3872.

ÖVER, S., ÜNLÜGENÇ, U. C. & BELLIER, O. 2002. Quaternary stress regime change in the Hatay region (SE Turkey). *Geophysics Journal International*, **148**, 649–662.

PARLAK, O., KOP, A., ÜNLÜGENÇ, U. C. & DEMIRKOL, C. 1998. Geochronology and geochemistry of basaltic rocks in the Karasu graben around Kırıkhan (Hatay), S. Turkey. *Turkish Journal of Earth Sciences*, **7**, 53–61.

PAYNE, A. S. & ROBERTSON, A. H. F. 1995. Neogene supra-subduction zone extension in the Polis graben system, west Cyprus. *Journal of the Geological Society, London*, **152**(4), 613–628.

PERINÇEK, D. & ÇEMEN, İ. 1990. The structural relationship between the East Anatolian and Dead Sea fault zones in southeastern Turkey. *Tectonophysics*, **172**, 331–340.

PILIDOU, S., PRIESTLEY, K., JACKSON, J. & MAGGI, A. 2004. The 1996 Cyprus earthquake: a large, deep event in the Cyprean Arc. *Geophysical Journal International*, **158**(1), 85–97.

PIRAZZOLI, P. A., LABOREL, J., SALIÈGE, J. F., EROL, O., KAYAN, I. & PERSON, A. 1991. Holocene raised shorelines on the Hatay coasts (Turkey): palaeoecological and tectonic implications. *Marine Geology*, **96**, 295–311.

PIŞKIN, O., DELALOYE, M., SELÇUK, H. & WAGNER, J. 1986. Guide to Hatay Geology (SE Turkey). *Ofioliti*, **11**, 87–104.

REILINGER, R. E., MCCLUSKY, S. C., ORAL, M. B., KING, W. & TOKSÖZ, M. N. 1997. Global positioning system measurement of present-day crustal movements in the Arabian–African–Eurasia plate collision zone. *Journal of Geophysics Research*, **102**, 9983–9999.

RIGO DE RIGHI, M. & CORTESINI, A. 1964. Gravity tectonics in foothills structure belt of SE Turkey. *American Association of Petroleum Geologists Bulletin*, **48**, 1911–1937.

ROBERTSON, A. H. F. 1986. The Hatay Ophiolite (southern Turkey) in its eastern Mediterranean tectonic context; a report on some aspects of the field excursion. *Ofioliti*, **11**(2), 105–119.

ROBERTSON, A. H. F. 1998*a*. Mesozoic–Tertiary tectonic evolution of the easternmost Mediterranean area: integration of marine and land evidence. *In*: ROBERTSON, A. H. F., EMEIS, K.-C., RICHTER, C. & CAMERLENGHI, A. (eds) *Proceedings of the Oceean Drilling Program, Scientific Results, 160*. Ocean Drilling Program, Collage Station, TX, 723–782.

ROBERTSON, A. H. F. 1998*b*. Tectonic significance of the Eratosthenes Seamount: a continental fragment in the process of collision with a subduction zone in the eastern Mediterranean (Ocean Drilling Program Leg 160). *Tectonophysics*, **298**, 63–82.

ROBERTSON, A. H. F. 2002. Overview of the genesis and emplacement of Mesozoic ophiolites in the Eastern Mediterranean Tethyan region. *Lithos*, **65** (1–2), 1–67.

ROBERTSON, A. H. F. 2004. Development of concepts concerning the genesis and emplacement of Tethyan ophiolites in the Eastern Mediterranean and Oman regions. *Earth-Science Reviews*, **66**(3–4), 331–387.

ROBERTSON, A. H. F., EATON, S., FOLLOWS, E. J. & PAYNE, A. S. 1995. Depositional processes and

basin analysis of Messinian evaporites in Cyprus. *Terra Nova*, **7**, 233–253.

ROBERTSON, A. H. F., EATON, S., FOLLOWS, E. J. & MCCALLUM, J. E. 1991. The role of local tectonics versus global sea-level change in the Neogene evolution of the Cyprus active margin. *In*: MACDONALD, D. I. M. (ed.) *Sedimentation, Tectonics and Eustasy: Sea-level Changes at Active Margins*. International Association of Sedimentologists, Special Publications, **12**, 331–369.

ROBERTSON, A. H. F., ÜNLÜGENÇ, U. C., İNAN, N. & TAŞLI, K. 2004. The Misis–Andırın Complex: a Mid-Tertiary mélange related to late-stage subduction of the Southern Neotethys in S Turkey. *Journal of Asian Earth Sciences*, **22**, 413–453.

ROJAY, B., HEIMANN, A. & TOPRAK, V. 2001. Neotectonic and volcanic characteristics of the Karasu fault zone (Anatolia, Turkey): the transition zone between the Dead Sea transform and the East Anatolian fault zone. *Geodinamica Acta*, **14**, 197–212.

ŞAFAK, Ü. 1993*a*. Antakya Havzası planktonic foraminifer biyostratigrafisi. (Planktonic Foraminifera biostratigraphy of Antakya Basin.) *Ankara Suat Erk jeoloji simpozyumu*, Ankara University, Ankara, 143–156.

ŞAFAK, Ü. 1993*b*. Antakya Havzası ostrakod foraminifer biyostratigrafisi. (The ostracode biostratigraphy of the Antakya Basin). *Geological Bulletin of Turkey*, **36**, 115–137 (in Turkish, with English abstract).

SALLER, A., ARMIN, R., ICHRAM, L. O. & SULLIVEN, C. 1993. Sequence stratigraphy of aggrading and backstepping carbonate shelves, Oligocene, Central Kalmantan, Indonesia. *In*: *Carbonate Sequence Stratigraphy: Recent Developments and Applications*. *In*: LOUCKS, R. G. & SARG, J. F. (eds) *Carbonate Sequence Stratigraphy—Recenr Events and Applications*. AAPG Memoirs, **57**, 267–290.

SALVINI, F. 2001. *Daisy 2.4: the structural data integrated system analyser*. University 'Roma Tre', Rome.

ŞAROĞLU, F., EMRE, Ö. & KUSÇU, İ. 1992. The East Anatolian fault zone of Turkey. *Annales Tectonicae*, **6**, 99–125.

SCHREIBER, B. C., FRIEDMAN, G. M., DECIMA, A. & SCREIBER, E. 1976. Depositional environments of upper Miocene (Messinian) evaporite deposition of the Sicilian basin. *Sedimentology*, **23**, 729–760.

ŞENGÖR, A. M. C. & KIDD, W. S. F. 1979. Post-collisional tectonics of the Turkish–Iranian plateau and a comparison with Tibet. *Tectonophysics*, **55**, 361–376.

ŞENGÖR, A. M. C., GÖRÜR, N. & ŞAROĞLU, F. 1985. Strike-slip faulting and related basin formation in zones of tectonic escape: Turkey as a case study. *In*: BIDDLE, K. T. & CHRISTIE, BLICK, N. (eds) *Strike-slip Deformation, Basin Formation and Sedimentation*. Society of Economic Paleontologists and Mineralogists, Special Publications, **37**, 227–264.

SENGÖR, A. M. C., TÜYSÜZ, O., IMREN, C., *et al.* 2005. The North Anatolian Fault: a new look. *Annual Review of Earth and Planetary Sciences*, **33**, 37–112.

SINCLAIR, H. D. 1997. Tectonstratigraphic model for underfilled peripheral foreland basins: an Alpine perspective. *Geological Society of America Bulletin*, **109**, 324–346.

STOCKMAL, G. S., BEAUMONT, C. & BOUTILIER, R. 1986. Geodynamic models of convergent margin tectonics: transition from rifted margin to overthrust belt and consequences for foreland-basin development. *American Association of Petroleum Geologists Bulletin*, **70**(2), 181–190.

TEN VEEN, J. H. & KLEINSPEHN, K. L. 2002. Geodynamics along an increasingly curved convergent plate margin: Late Miocene–Pleistocene Rhodes, Greece. *Tectonics*, **21**(3), 1017–1038.

TINKLER, C., WAGNER, J. J., DELALOYE, M. & SELÇUK, H. 1981. Tectonic history of the Hatay Ophiolites (South Turkey) and their relationship with the Dead Sea rift. *Tectonophysics*, **72**, 23–41.

TRON, V. & BRUN, J.-P. 1991. Experiments on oblique rifting in brittle–ductile systems. *Tectonophysics*, **188**, 71–84.

UMHOEFER, P. J. & STONE, K. A. 1996. Description and kinematics of the SE Loreto basin fault array, Baja California Sur, Mexico: a positive field test of oblique-rift models. *Journal of Structural Geology*, **18**, 595–614.

VEEVERS, J. J., FALVEY, D. A. & ROBINS, S. 1978. Timor Trough and Australia: facies show topographic wave migrated 80 km during the past 3 myr. *Tectonophysics*, **45**, 217–227.

WESTAWAY, R. 1994. Present day kinematics of the Middle East and Eastern Mediterranean. *Journal of Geophysical Research*, **99**, 12071–12090.

WESTAWAY, R. & ARGER, J. 1996. The Gölbaşı basin, southeastern Turkey: a complex discontinuity in a major strike-slip zone. *Journal of the Geological Society, London*, **153**, 729–743.

WITHJACK, M. O. & JAMIESON, W. R. 1986. Deformation produced by oblique rifting. *Tectonophysics*, **126**, 99–124.

YETIŞ, C. 1978. Geology of the Amardi (Niğde) region and the characteristics of the Ecemiş Fault Zone between Madan Boğazı and Kamişli. *Istanbul University Fen Fakultesi Mecanik Series B*, **43**, 41–61.

YILMAZ, Y. 1993. New evidence and model on the evolution of the southeast Anatolian orogen. *Geological Society of America Bulletin*, **105**(2), 251–271.

YURTMEN, S., HERVÉ, G., WESTAWAY, R., ROWBOTHAM, G. & TATAR, O. 2002. Rate of strike-slip motion on the Amanos Fault (Karasu Valley, southern Turkey) constrained by K–Ar dating and geochemical analysis of Quaternary basalts. *Tectonophysics*, **344**, 207–246.

YÜRÜR, T. & CHOROWICZ, J. 1998. Recent volcanism, tectonics and plate kinematics near the junction of the African, Arabian and Anatolian plates in the Eastern Mediterranean. *Journal of Volcanology and Geothermal Research*, **85**, 1–15.

ZANCHI, A. CROSTA, G. B. & DARKAL, A. N. 2002. Palaeostress analysis in NW Syria: constraints on the Cenozoic evolution of the northwestern margin of the Arabian plate. *Tectonophysics*, **357**, 255–278.